



CRIPAC
智能感知与计算研究中心
Center for Research on Intelligent
Perception and Computing



A Lightweight Multi-label Segmentation Network for Mobile Iris Biometrics

Caiyong Wang^{1,2}, Yunlong Wang², Boqiang Xu^{1,2}, Yong He², Zhiwei Dong³, Zhenan Sun^{1,2}, ✉

¹School of Artificial Intelligence, University of Chinese Academy of Sciences, China

²CRIPAC, NLPR, CASIA, China

³University of Science and Technology Beijing, China

caiyong.wang@cripac.ia.ac.cn, znsun@nlpr.ia.ac.cn

Outline

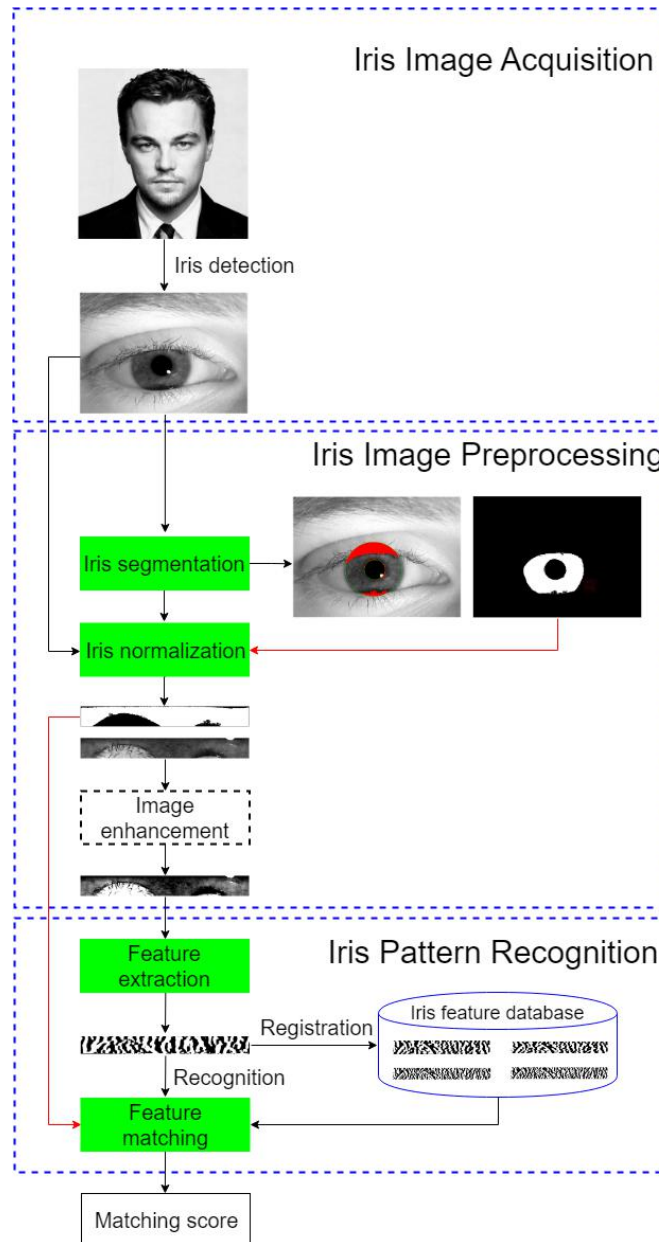
Background

Proposed Method

Experimental Results

Conclusion

➤ Iris recognition



➤ Iris recognition

■ Hamming distance

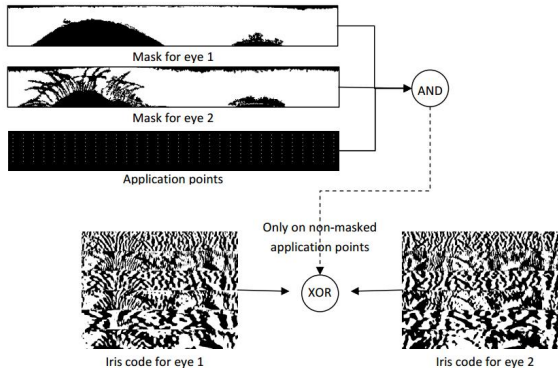
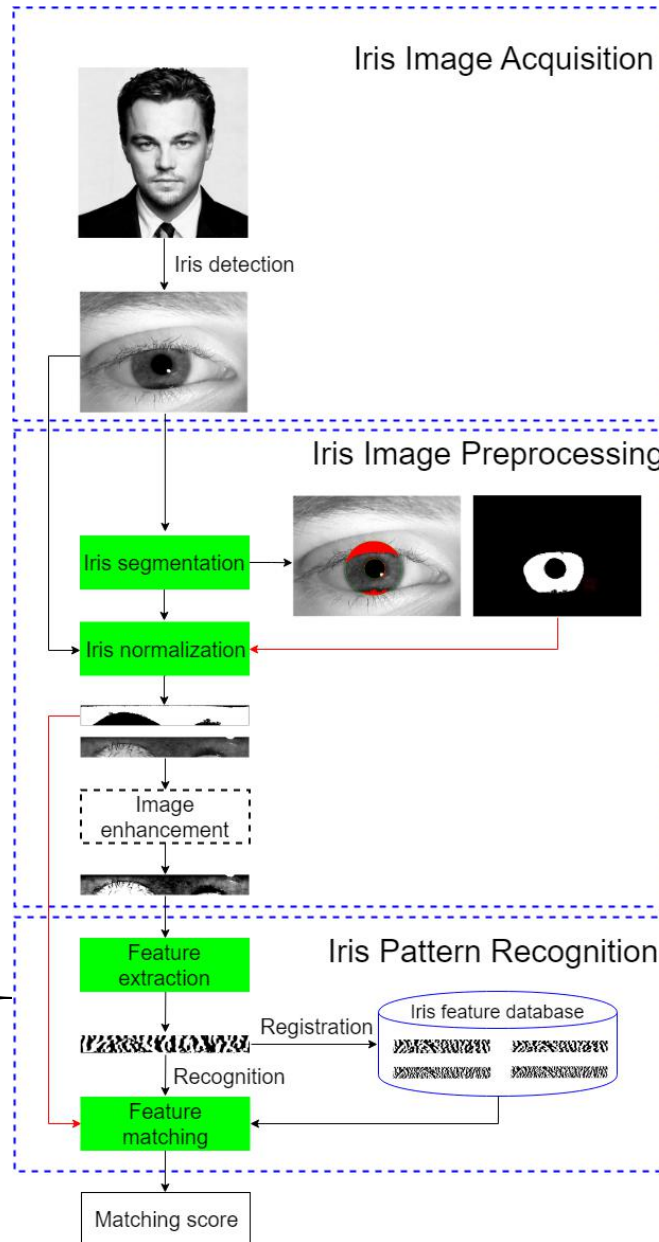


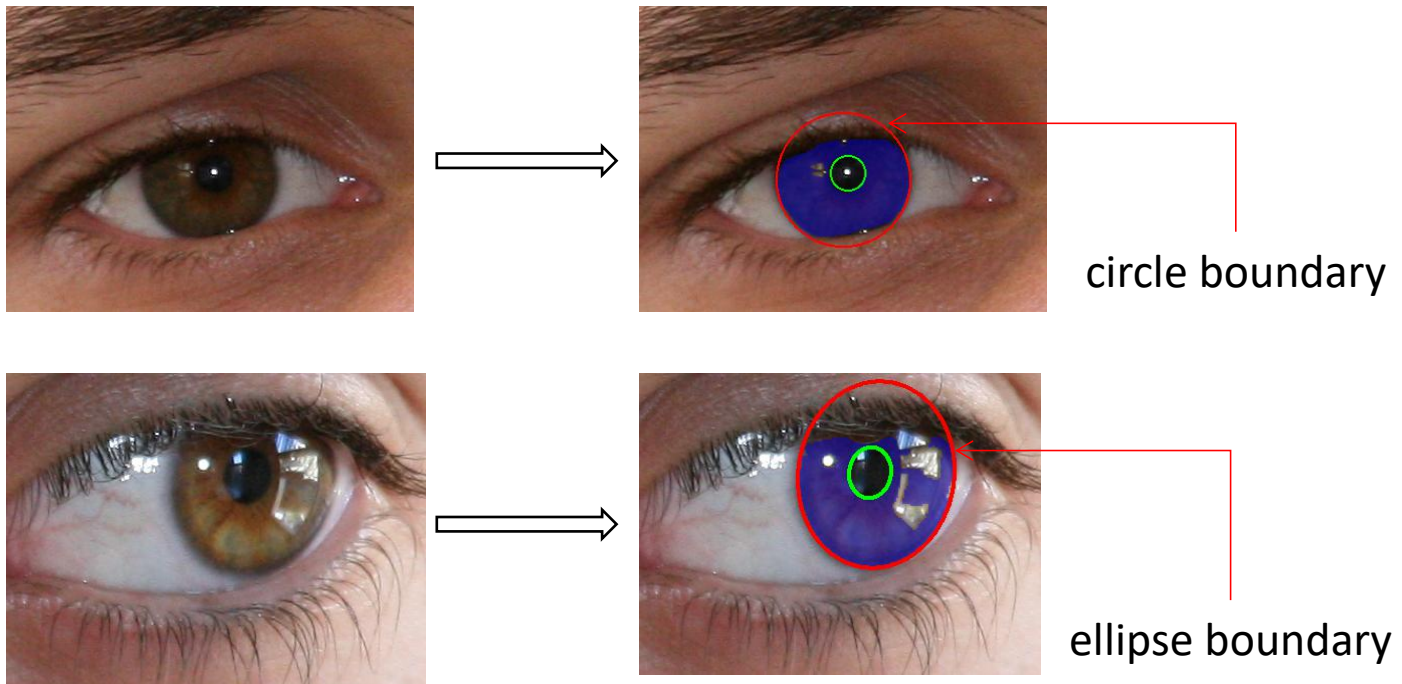
Figure 16: The XOR operator is used to compare two iris codes. Only the non-masked application points are considered during the XOR operation

Only the **non-masked application points** are considered during the XOR operation.



➤ Iris segmentation (Complete)

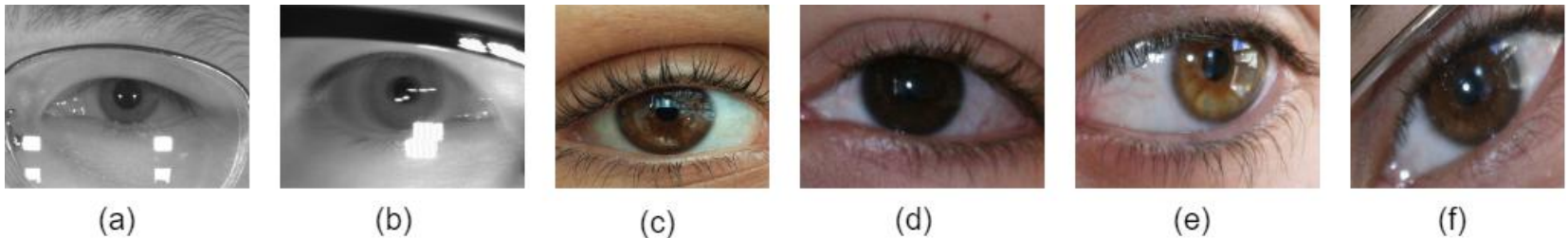
- ❖ Segmentation of iris noisy mask (Optional)
- ❖ Localization of **parameterized** iris inner and outer boundaries



➤ Iris segmentation on mobile devices

■ An ideal iris segmentation method on mobile devices should be:

❖ Accurate, Robust to noise

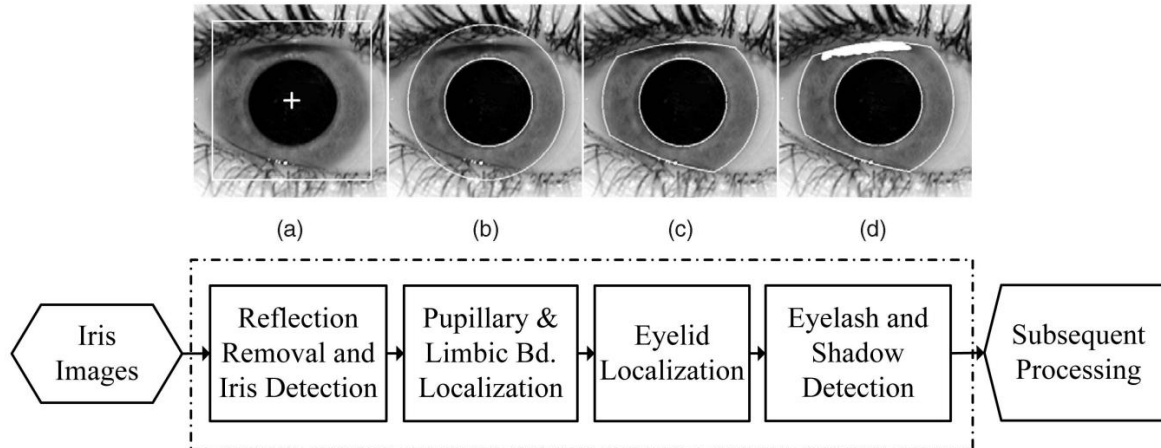


(a) glass and reflection; (b) motion blur; (c) specular reflection; (d) dark iris; (e) off angle; (f) rotated iris.

❖ Lightweight, fast

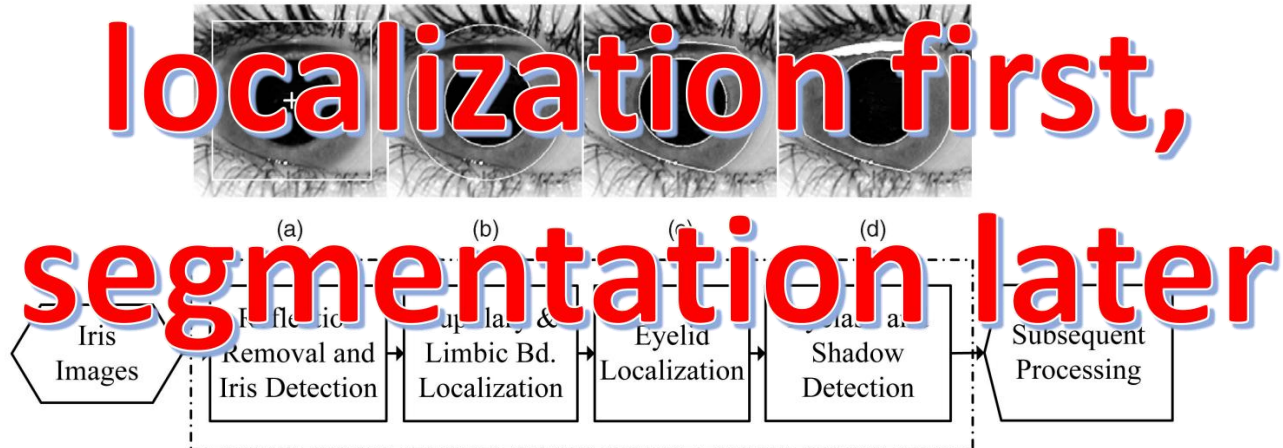
- ✓ It should consider the limited resource of computing and storage of mobile devices.
- ✓ It should be fast (real-time) for accelerating recognition process.

➤ Two typical iris segmentation methods



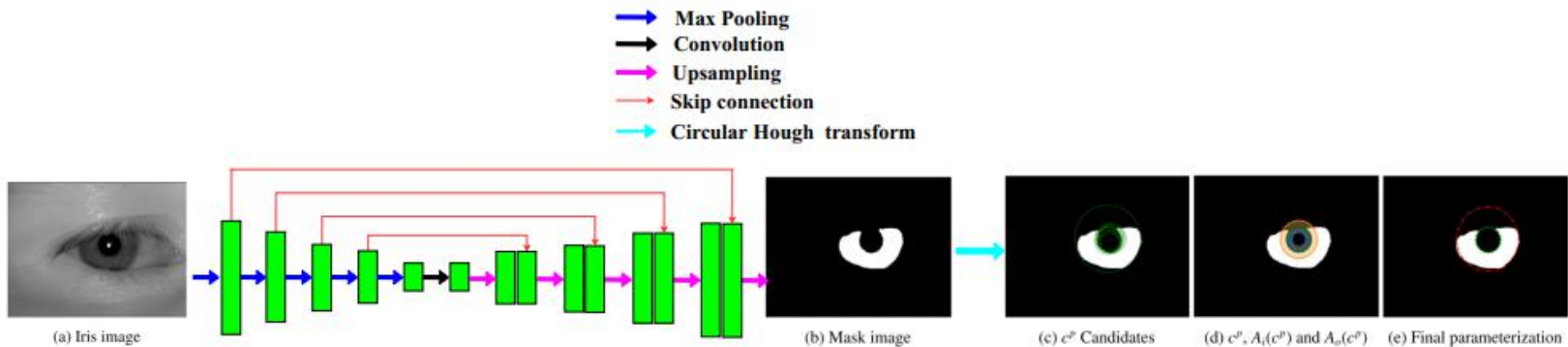
Z. He, T. Tan, Z. Sun, and X. Qiu, "Toward accurate and fast iris segmentation for iris biometrics," IEEE Transactions on Pattern Analysis and Machine Intelligence, vol. 31, no. 9, pp. 1670–1684, 2008.

➤ Two typical iris segmentation methods



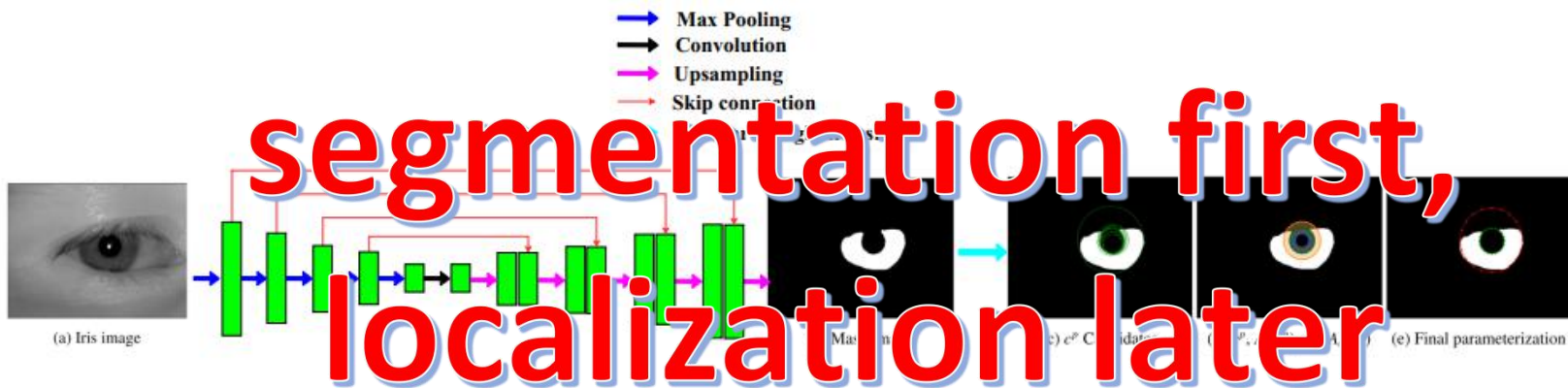
Z. He, T. Tan, Z. Sun, and X. Qiu, "Toward accurate and fast iris segmentation for iris biometrics," IEEE Transactions on Pattern Analysis and Machine Intelligence, vol. 31, no. 9, pp. 1670–1684, 2008.

➤ Two typical iris segmentation methods



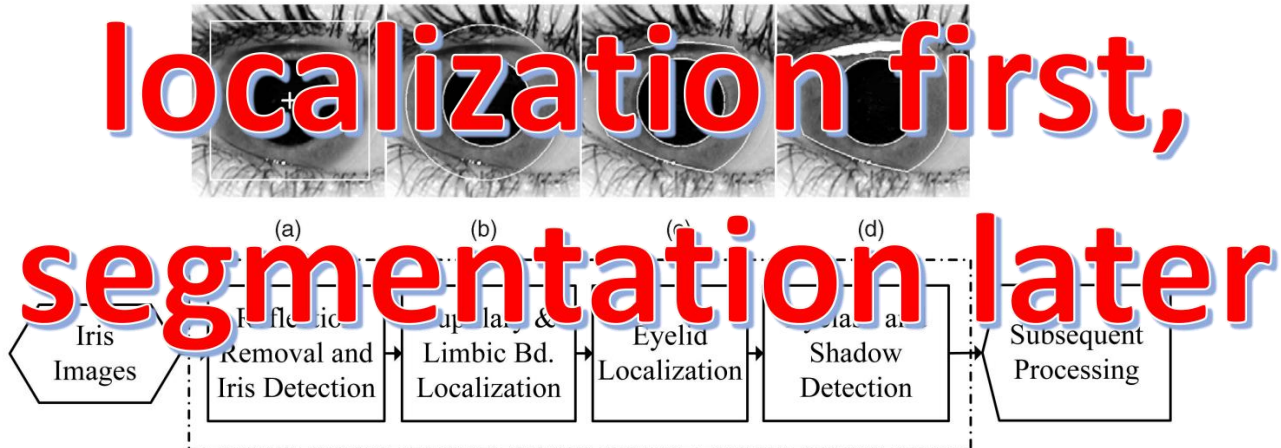
H. Hofbauer, E. Jalilian, and A. Uhl, "Exploiting superior cnn-based iris segmentation for better recognition accuracy," Pattern Recognition Letters, vol. 120, pp. 17–23, 2019. [CNNHT]

➤ Two typical iris segmentation methods

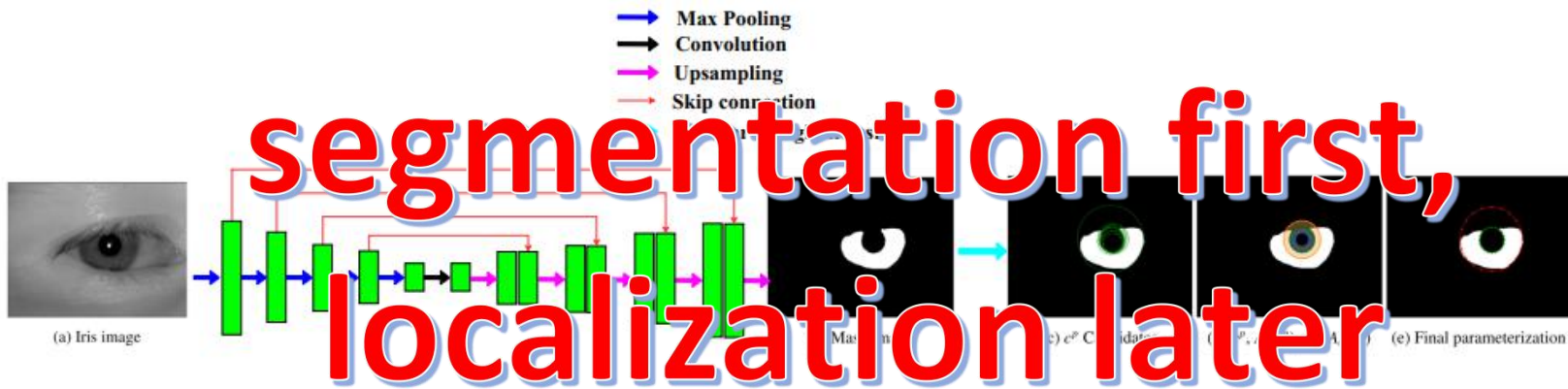


H. Hofbauer, E. Jalilian, and A. Uhl, "Exploiting superior cnn-based iris segmentation for better recognition accuracy," Pattern Recognition Letters, vol. 120, pp. 17–23, 2019. [CNNHT]

➤ Two typical iris segmentation methods

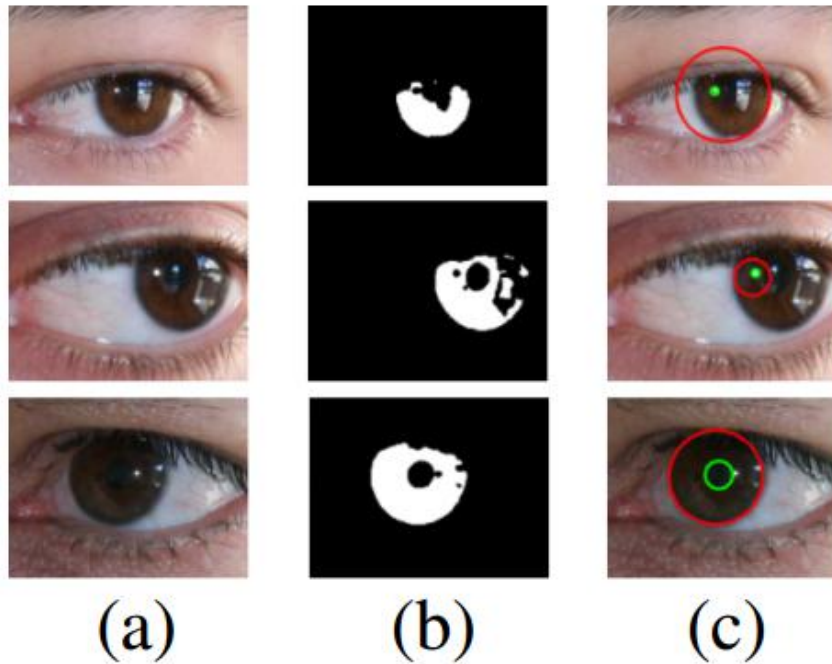


Z. He, T. Tan, Z. Sun, and X. Qiu, "Toward accurate and fast iris segmentation for iris biometrics," IEEE Transactions on Pattern Analysis and Machine Intelligence, vol. 31, no. 9, pp. 1670–1684, 2008.



H. Hofbauer, E. Jalilian, and A. Uhl, "Exploiting superior cnn-based iris segmentation for better recognition accuracy," Pattern Recognition Letters, vol. 120, pp. 17–23, 2019. [CNNHT]

➤ Failure samples of CNNHT



- ◆ CNNHT is easy to fail when confronted with highly irregular or extremely noisy segmentation masks.
- ◆ CNNHT also takes a large amount of time on searching for optimal iris boundary parameters.

Outline

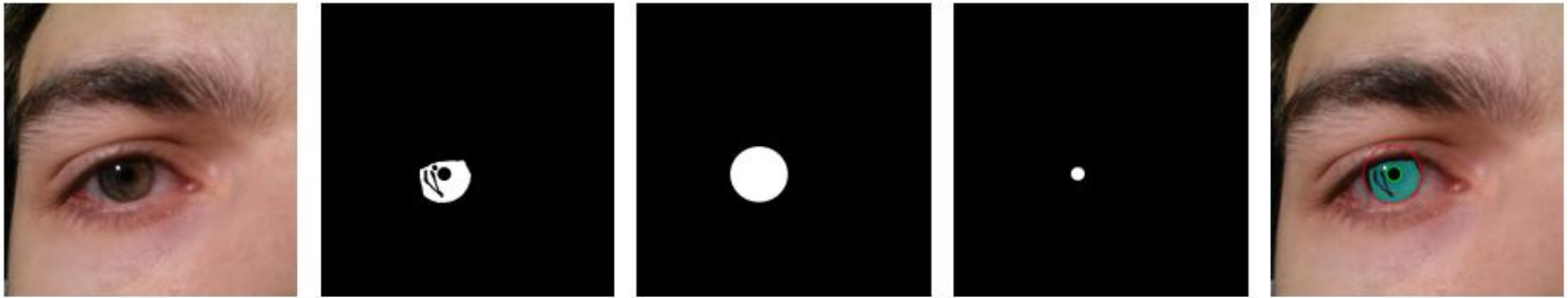
Background

Proposed Method

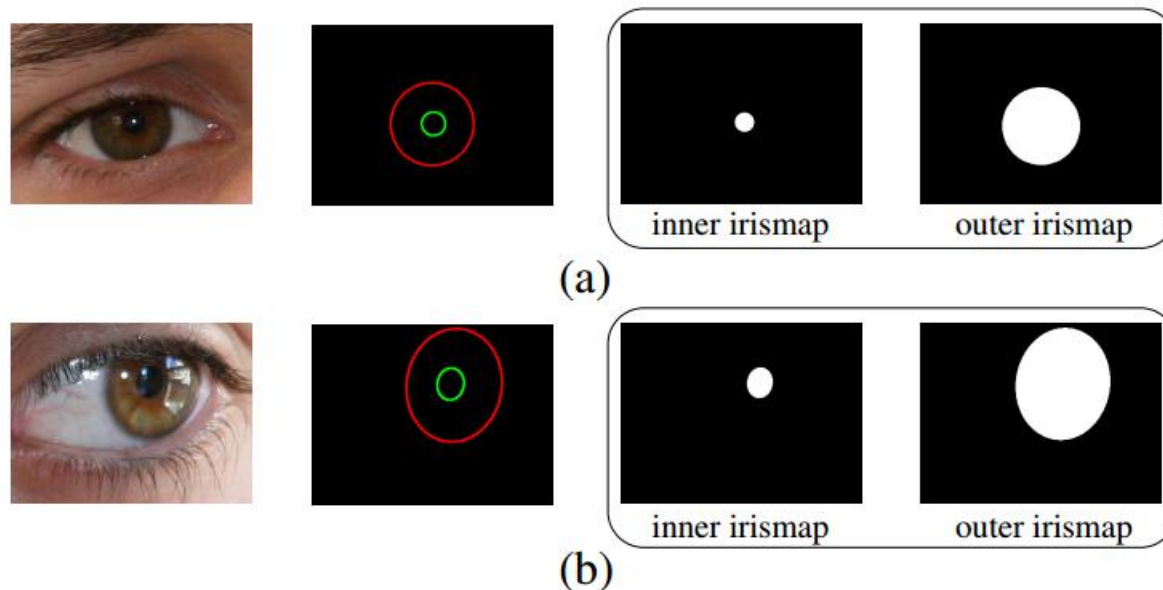
Experimental Results

Conclusion

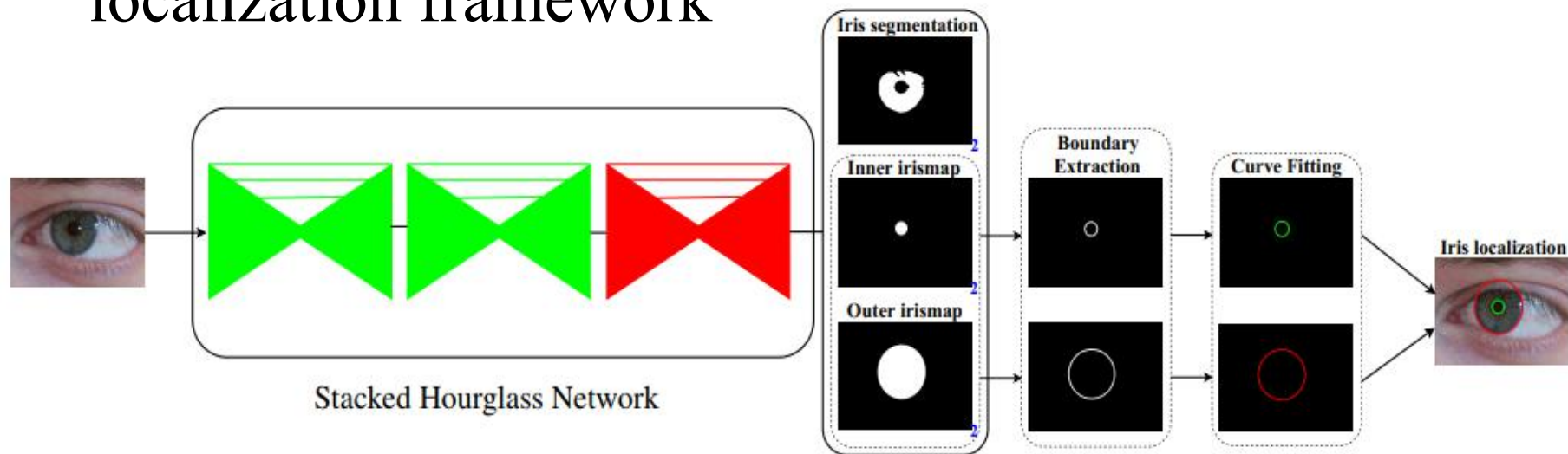
➤ Multi-label learning



- ❖ Iris mask, inner irismap, and outer irismap are overlapping from each other.
- ❖ The model needs to assign each pixel to multiple binary labels.



➤ The proposed unified iris segmentation and localization framework



➤ Lightweight stacked hourglass network

- ❖ The stride of the initial convolutional layer with kernel size 7×7 is changed from 2 to 1.
- ❖ The initial max-pooling layer is removed.
- ❖ The per-layer channel number of the network is reduced from 256 to 64.
- ❖ Each hourglass module is processed at 4 different image scales, and stacked 3 times.

➤ Multi-label loss function

$$\mathcal{L} = \lambda_1 \mathcal{L}_{seg} + \lambda_2 \mathcal{L}_{inner} + \lambda_3 \mathcal{L}_{outer}$$

- ❖ $\mathcal{L}_{seg}, \mathcal{L}_{inner}, \mathcal{L}_{outer}$ are implemented as cross-entropy loss over two classes (foreground vs. background).
- ❖ The coefficients λ_1, λ_2 and λ_3 are all set to 1 to make these loss value ranges comparable.
- ❖ The loss is applied to the output of the last hourglass module without intermediate supervision.

Outline

Background

Proposed Method

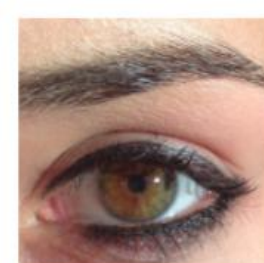
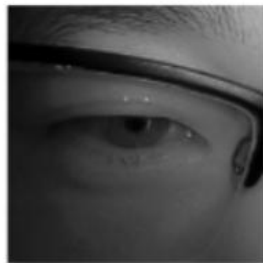
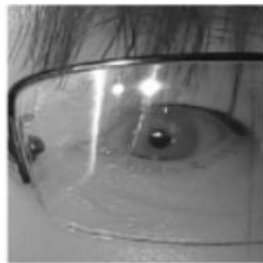
Experimental Results

Conclusion

➤ Experimental Settings

❖ Database:

Database	Illuminati on	Resoluti on	Training set	Testing set
CASIA-Iris- M1	NIR	400×400	1500	1500
MICHE-I	VIS	Various	680	191



CASIA-Iris-M1-S1

CASIA-Iris-M1-S2

CASIA-Iris-M1-S3

MICHE-I

➤ Experimental Settings

❖ Evaluation Protocols:

- Iris segmentation (from NICE.I competition)

$$E1 = \frac{1}{n \times c \times r} \sum_{c'} \sum_{r'} G(c', r') \otimes M(c', r')$$

which evaluates the inconsistent pixels between G and M.

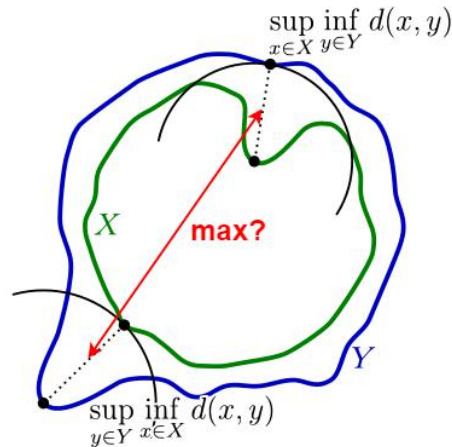


The value of E1 is bounded in [0,1], where the ***smaller value*** indicates the ***better segmentation*** result.

➤ Experimental Settings

❖ Evaluation Protocols:

- Iris localization (from Hausdorff distance)



$$H(G, B) = \max \left\{ \sup_{x \in G} \inf_{y \in B} \|x - y\|, \sup_{y \in B} \inf_{x \in G} \|x - y\| \right\}$$

which measures the shape similarity between the predicted iris inner or outer boundaries and its ground truth.



Smaller Hausdorff distances correspond to ***higher shape similarity*** between predicted iris boundary and its ground truth, suggesting ***higher detection accuracy***.



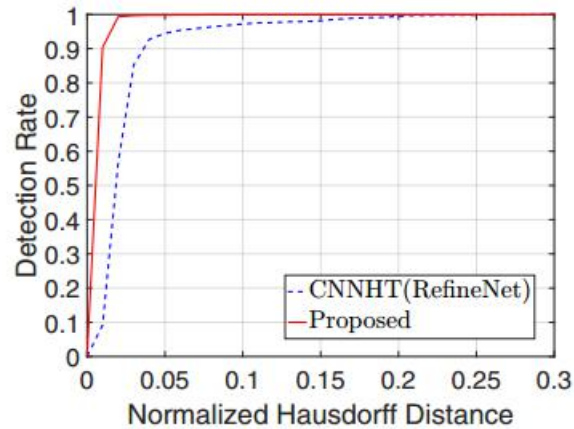
Percentage of Correct Localization (PCL) curve, AUC@ τ about varying distance threshold

➤ Experimental Results

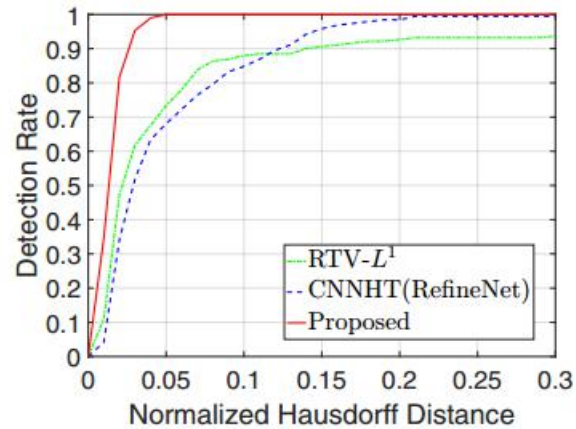
Method	Database	$E1$ (%)	Overall	
			mHdis (%)	AUC@0.3
RTV- L^1 [20]	MICHE-I	2.42	4.3852	0.2522
MFCNs [4]	CASIA-Iris-M1	0.77	N/A	N/A
	MICHE-I	0.74	N/A	N/A
CNNHT [7] (RefineNet)	CASIA-Iris-M1	0.71	1.7245	0.2803
	MICHE-I	0.80	3.6824	0.2559
Proposed	CASIA-Iris-M1	0.72	0.5517	0.2987
	MICHE-I	0.82	1.1107	0.2910

Table 1. Comparison of iris segmentation and localization (circular boundary) for different approaches.

➤ Experimental Results



(a) CASIA-Iris-M1

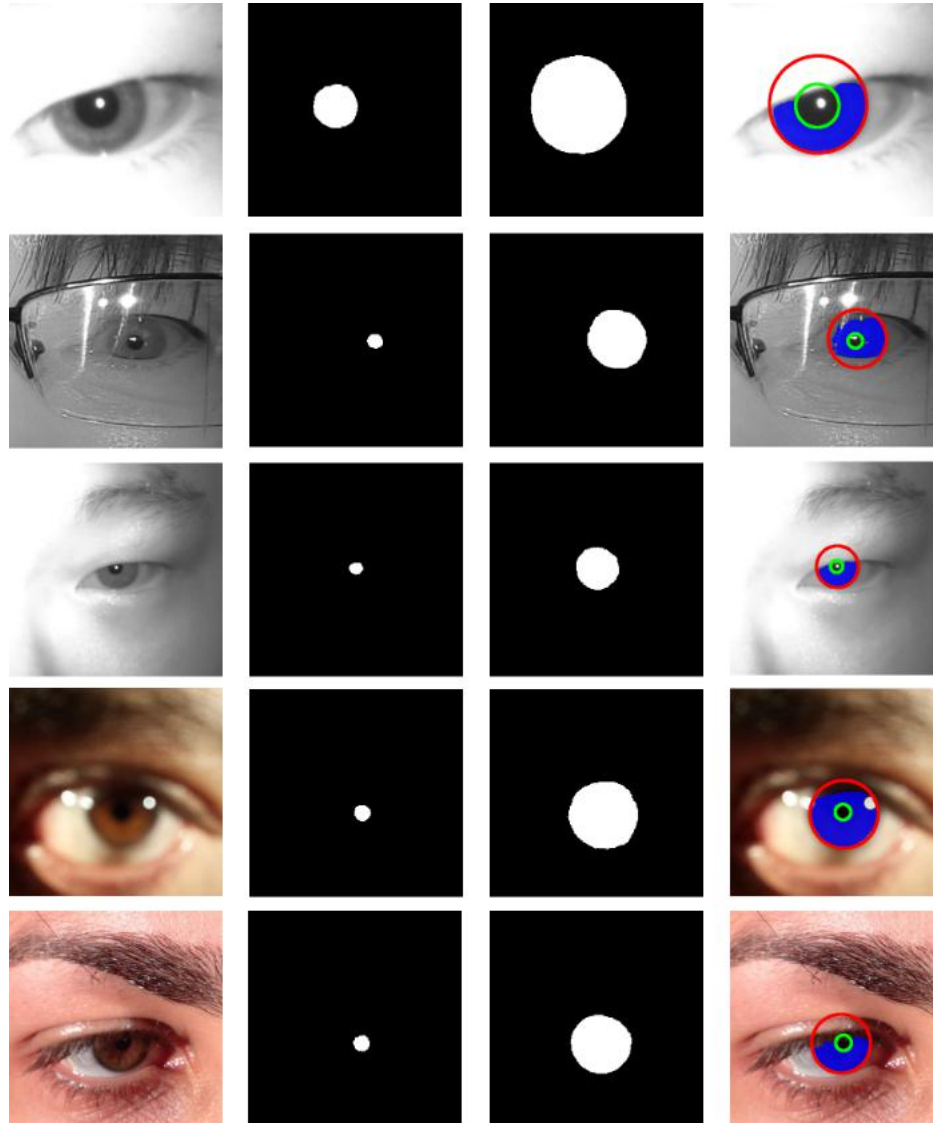


(b) MICHE-I

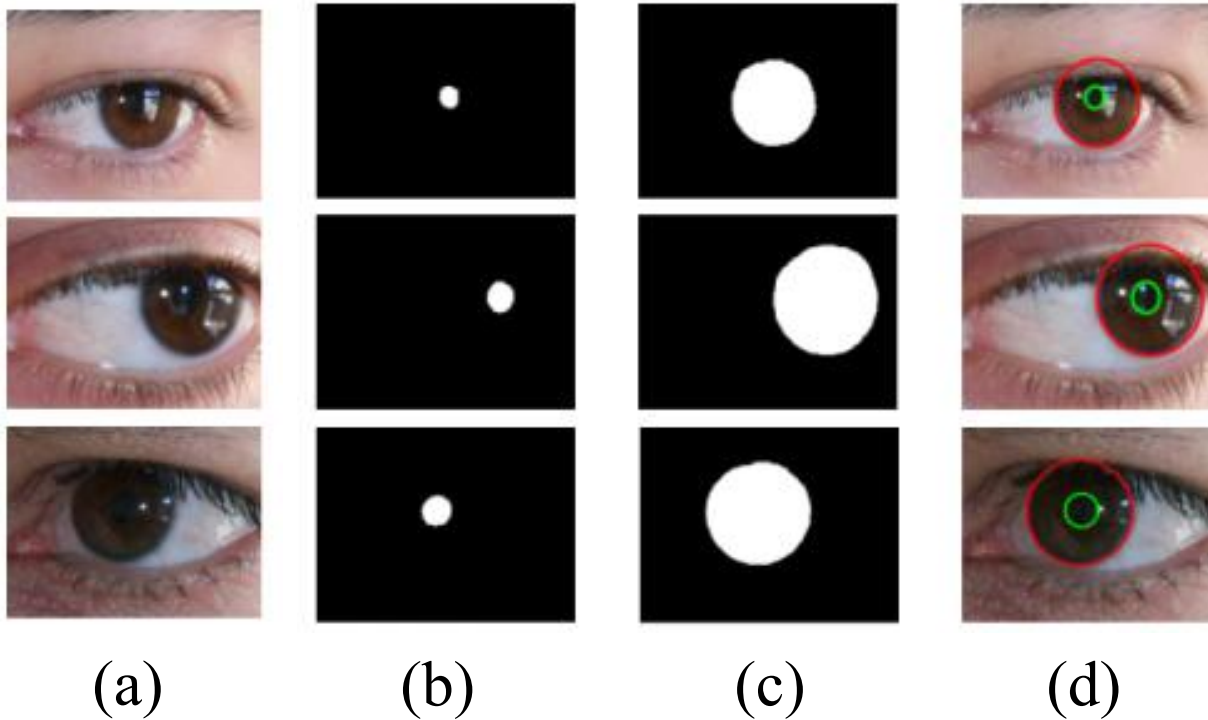
Fig. 3. Comparison of iris localization for different approaches using the proposed PCL curve.

- ✓ For iris segmentation, the proposed method achieves comparable results ***compared with the current state-of-the-art method.***
- ✓ For iris localization, the proposed method ***consistently outperforms other methods*** by a large margin in all metrics across all databases.

➤ Experimental Results



➤ Experimental Results



- ✓ The proposed method ***makes full use of the original iris images to learn complete inner and outer iris boundaries*** so it can achieve much more robust and accurate iris localization results.

➤ Model complexity

Method	Params (M)	FLOPs (G) [†]	Storage (MB)
MFCNs [4]	21.68	156.35	82.70
CNNHT(RefineNet) [7]	61.87	144.79	236.00
Proposed	0.69	74.27	2.83

[†] The FLOPs is calculated with the resolution of 640×480 .

Table 2. Comparison of model complexity for different approaches.

- ✓ The proposed model is lightweight and high-efficiency.

Outline

Background

Proposed Method

Experimental Results

Conclusion

➤ Conclusion

- ✓ This paper proposes a ***lightweight multi-label learning*** framework for ***complete iris segmentation*** on mobile devices.
- ✓ The proposed method achieves ***competitive or state-of-the-art performance*** in ***both iris segmentation and localization*** on two challenging mobile iris datasets.

➤ References

1. Z. He, T. Tan, Z. Sun, and X. Qiu, "Toward accurate and fast iris segmentation for iris biometrics," *IEEE Transactions on Pattern Analysis and Machine Intelligence*, vol. 31, no. 9, pp. 1670–1684, 2008.
2. H. Hofbauer, E. Jalilian, and A. Uhl, "Exploiting superior cnn-based iris segmentation for better recognition accuracy," *Pattern Recognition Letters*, vol. 120, pp. 17–23, 2019.
3. C. Wang, J. Muhammad, Y. Wang, Z. He and Z. Sun, "Towards Complete and Accurate Iris Segmentation Using Deep Multi-Task Attention Network for Non-Cooperative Iris Recognition," in *IEEE Transactions on Information Forensics and Security*, vol. 15, pp. 2944-2959, 2020.



CRIPAC

智能感知与计算研究中心

Center for Research on Intelligent
Perception and Computing

Thank you!